minerals

MDPI

Article

Mortars from the Palace of Knossos in Crete, Greece: A Multi-Analytical Approach

Fernanda Carvalho [1,2,*], Pedro Sousa [2], Nuno Leal [3], Joaquim Simão [3], Elissavet Kavoulaki [4], Maria Margarida Lima [1,2], Teresa Pereira da Silva [5], Hugo Águas [1,2], Giuseppina Padeletti [6] and João Pedro Veiga [1,7]

1 CENIMAT/I3N—Centro de Investigação de Materiais, NOVA School of Science & Technology—FCT NOVA, 2829-516 Caparica, Portugal; mmal@fct.unl.pt (M.M.L.); hma@fct.unl.pt (H.Á.); jpv@fct.unl.pt (J.P.V.)
2 Department of Materials Science, NOVA School of Science & Technology—FCT NOVA, 2829-516 Caparica, Portugal; pf.sousa@campus.fct.unl.pt
3 GEOBIOTEC and Earth Sciences Department, NOVA School of Science & Technology—FCT NOVA, 2803-516 Caparica, Portugal; n.leal@fct.unl.pt (N.L.); jars@fct.unl.pt (J.S.)
4 EPHORATE of Antiquities of Heraklion, Xanthoudidou & 1 Chatzidaki Str, 71202 Heraklion, Greece; ekavoulaki@culture.gr
5 LNEG—Laboratório Nacional de Energia e Geologia, I.P., Unidade de Recursos Minerais e Geofísica, Apt. 7586, 2610-999 Amadora, Portugal; teresa.pena@lneg.pt
6 CNR Consiglio Nazionale delle Ricerche, ISMN—Instituto per lo Studio dei Materiali Nanostrutturati, 10 Via Salaria km 29.5, 00015 Monterotondo, Italy; giuseppina.padeletti@cnr.it
7 Department of Conservation and Restoration, NOVA School of Science & Technology—FCT NOVA, 2829-516 Caparica, Portugal
* Correspondence: fb.carvalho@campus.fct.unl.pt

check for updates

Citation: Carvalho, F.; Sousa, P.; Leal, N.; Simão, J.; Kavoulaki, E.; Lima, M.M.; da Silva, T.P.; Águas, H.; Padeletti, G.; Veiga, J.P. Mortars from the Palace of Knossos in Crete, Greece: A Multi-Analytical Approach. *Minerals* **2022**, *12*, 30. https://doi.org/10.3390/min12010030

Academic Editors: Daniele Moro and Jordi Ibanez-Insa

Received: 4 November 2021
Accepted: 21 December 2021
Published: 24 December 2021

Abstract: The study of building materials constituting cultural heritage is fundamental to understand their characteristics and predict their behavior. When considering materials from archaeological sites, their characterization can provide not only relevant information for a broader understanding of the site and its importance and significance but can also increase knowledge about ancient materials and their performance. The Palace of Knossos is a very important archaeological site in the European history context, and its preservation benefits from the characterization of the constituent materials. Samples of mortars from this monument were collected under the scope of the H2020 HERACLES project, where a multi-analytical approach was chosen using established protocols for the different sample typologies. Instrumental techniques such as optical microscopy (OM), X-ray diffraction (XRD), Fourier-transform infrared spectroscopy (FTIR), and simultaneous thermogravimetry and differential thermal analysis (TG–DTA) were used for the chemical, mineralogical, and morphological characterization of these mortar samples. The results indicate that the majority are lime mortars, both aerial and hydraulic, but gypsum-based mortars were also identified. Differences in the chemical composition of the samples in distinct areas of the monument allowed us to reflect on the variety of materials used in the construction of the Palace of Knossos.

Keywords: mortars; binders; built heritage; characterization; Palace of Knossos

1. Introduction

The European built cultural heritage consists of a vast set of unique monuments of incalculable value, constituting a fingerprint of our common history and cultural identity. Their importance to the community goes far beyond a local interest, fundamentally contributing, directly and indirectly, to the development of the region where they are inserted. The relevance of this built heritage requires periodic maintenance actions of both the monument and eventual works of adaptation, to better preserve them in situ, and to better meet the modern requirements of safety and comfort of visitors. Environmental and meteorological phenomena such as rainwater, wind, temperature variations, or relative humidity can strongly affect built cultural heritage and consequently its integrity [1,2].

Some of these questions were dealt with in the HEritage Resilience Against CLimate Events on Site (HERACLES) project [3,4] promoting practices to increase the resilience of built heritage facing climate effects.

The development of materials used for construction sought to meet criteria of durability and resistance, although they are not immune to the natural wear and tear of time and environment. In this context, mortars are an element of relevance, due to their possible different functions in a construction. They can assume a structural function as the bedding of stonework, a protection function of the structure when applied as renders, as a fixing element of coatings, a finishing and/or decoration element [5,6]. Each of these functions require distinct characteristics achieved through the selection of raw materials, the ratio between binder and aggregate, along with the preparation and application of these mortars. Regardless of its function, the process of preparation is quite simple, consisting mainly of the mixture of the binder and the aggregate with water, giving plasticity to the resultant material, essential to the application of the mortars. However, the mineralogical nature of the main components, as well as their physical features, are determinant for the adequacy of mortar properties and characteristics [6–9]. Binders and aggregates have been used over the centuries and, depending on the availability of raw materials, they can have varied compositions [10]. The most used binders in ancient mortars are clay, gypsum, and lime, a historical prevalence existing in the use of the latter [6,8,10].

1.1. Lime-Based Mortars: Binders and Aggregates

Lime (CaO) has its origin in the calcination of calcium carbonate ($CaCO_3$), from limestones or other $CaCO_3$-rich rocks. In this process, heating limestone at a temperature close to 900 °C causes the dissociation of calcium carbonate into calcium oxide (CaO) and carbon dioxide (CO_2) [11,12]. The rock used in this calcination process is determinant for the type of binder obtained and can lead to limes with different properties. More or less pure carbonated rocks, with high calcite and/or dolomite contents, give rise to air lime, while impure carbonated rocks, which may include clay minerals or the addition of pozzolanic components, give rise to natural hydraulic lime [13]. The lime resulting from the calcination process of purer rocks, known as quick lime, is an unstable component and usually needs to be hydrated before the preparation of the mortar. The hydration process of quick lime can give rise to both portlandite ($Ca(OH)_2$) in the case of limestones, and brucite ($Mg(OH)_2$) when dolomite is the calcined rock. Once the mortar is prepared with this type of binder, the carbonation process occurs due to the CO_2 present in the air, which reacts with the calcium hydroxide of the mortar to form calcium carbonate ($CaCO_3$), hence this type of lime being also known as air lime [12]. Mortars prepared with natural hydraulic lime, or air-hardening lime with pozzolanic additives, such as volcanic ash, tuffs, and ground ceramics, among other components, involve chemical processes in which water promotes the reaction of these minerals with portlandite and the precipitation of new mineral phases (calcium and aluminosilicates, for example), which results in the hardening of the mortar. For this reason, this type of binder is known as hydraulic lime [6,12,14,15].

Although the mortars are defined by the binder used, the aggregates play a fundamental role in the properties of this material, being decisive for its strength and durability. Particle size, the mineralogical composition, and shape of the grains interfere in aggregate interaction with the binder, in the porosity and in the amount of water ideal for the preparation of the mortar. The addition of aggregates can also limit the intensity of retraction of the mortar during the carbonation process [9,12,16–18]. Regarding the shape of aggregates, prevalence of rounded grains promotes larger pores in the structure of the mortar and can reduce the mechanical strength of the material. However, if rounded grains have a heterogeneous size distribution, that is to say that large, medium, and small-sized grains occur, mechanical strength will increase as pores will become smaller. Angled and irregular-shaped grains promote a network of smaller pores and better adhesive properties on the support materials, promoting a better resistance of the mortar [9,12]. Considering the particle size, mortars with coarser aggregates contribute to their volumetric stability [17].

Mortars with finishing functions are applied in several layers, in which the mixed aggregates range from coarser particles used in the layers applied next to the support, to thinner aggregates in the more superficial layers, which favor a smoother and more compact application [19,20]. Regarding mineralogy, silicate sand, in most cases mainly composed of quartz, and carbonated sands are the most common, although other minerals may be part of the aggregate composition. Quartz contributes mainly to the chemical resistance of the mortar while carbonated aggregates contribute to the carbonation process, promoting an increase in density and mechanical resistance, notably in aerial lime mortars [6,12,18,21].

This mineral diversity and all the variables that influence the properties and durability of these materials make the study of the chemical mineralogical and physical characteristics of historical mortars complex. When considering the historical context, it is important to keep in mind that most of the ancient mortars are the result of artisanal processes of raw materials extraction and processing, as well as preparation and application. Although this is not synonymous with poorly executed work or lack of quality, most samples come from buildings or monuments that have had different construction or reconstruction stages, or have undergone interventions over time, often undocumented [22]. Original mortars can be mixed with others produced in different contexts, hindering clear distinctions of characteristics to be grouped in certain historical periods. The wider and more diverse this type of study is, the greater the possibility of perceiving specific or regional issues that can assist in other types of study on mortars.

In this context, this work presents the results obtained specifically with the characterization of mortars from the Minoan Palace of Knossos. The samples studied correspond to materials applied with different functions, which will make it possible to understand and to interpret the particularities of each of these mortars.

1.2. The Case Study: The Palace of Knossos

The Palace of Knossos is a unique witness of the organization and development of the Minoan civilization, one of the first in Europe. In addition to its relevance as an archaeological site, its own history of preservation brings a vast wealth of materials. It occupies an approximate area of 22,000 m^2, being the largest Minoan palace built in Crete. It is located at 6 km to the SE of Heraklion city, close to the airport and the seashore line.

Despite being relatively close to the coast, the palace was built on top of the Kefala Hill, in an area between two rivers and topographically somewhat protected from the sea influence [4,23–25]. In addition to the favorable location, the geological characteristics of the island also determined the material resources used for the construction. Approximately 75% of the island of Crete surface is covered by carbonated rocks, and the Knossos region is composed mostly of Pliocene-, Miocene-, and Cretaceous-age limestones [26], while southwards, gypsum outcrops are found (Figure 1). Local rocks were the main source of raw materials for Minoan constructions. Mainly, Neogene-age limestones, as well as gypsum, were used, the latter also used as finishing in interior areas and as a coating material [25,27–29]. Furthermore, clays and wood were also employed in the construction.

The first palace was reportedly built around 2000 B.C. and destroyed centuries later around 1700 B.C. A new, more majestic palace built on the same site in this period again suffered various factors such as earthquakes, fire, and abandonment until it was definitively destroyed around 1400 B.C. [24,29,30]. However, the work carried out and the archaeological finds in the region reveal that Kefala Hill maintained its importance for many centuries.

The archaeological excavation work in this region was initiated at the end of the 19th century by Minos Kalokerinos, but it was Sir Arthur Evans who was the archaeologist responsible for most of the excavations carried out from 1900 and was greatly responsible for what is known today. The construction layout exposed with the excavations revealed structures built around a central courtyard, with distinct functions (see Figure 3). The western side would be dedicated to the spaces for warehouses and services and the East Wing of the palace would be dedicated to the royal quarters and housing area [25,29,31]. The Palace of Knossos was built in height and had several connecting structures between the different wings, such as corridors and stairs. In addition, its architecture favored water access, water drainage, air circulation, and natural lighting [24,25,30,31]. Among the structures discovered on the west side stands out the West Magazines, excavated completely by A. Evans in 1900. It is an area of more than 1000 m^2, divided into 18 physically similar warehouses, all of which are narrow and elongated spaces. The walls were built with stones and clay and some featured plasters with mortar and decoration. The area of these warehouses would have a cover, supported by horizontal and vertical wooden beams, positioned at relatively regular intervals, remaining marked on both sides of the walls [24,32]. On the east side of the Palace, excavations discovered several structures identified as rooms, among which are the royal rooms. In addition to these, some rooms for storage and worship have also been identified. Because this is the steeper area of the terrain, it was in the East Wing that A. Evans found a large staircase, in addition to other preserved structures such as the drainage system and exterior walls [33]. In several of these rooms, slabs of mineral gypsum was found, used as wall and floor coverings, as well as in fragments of mural paintings [34].

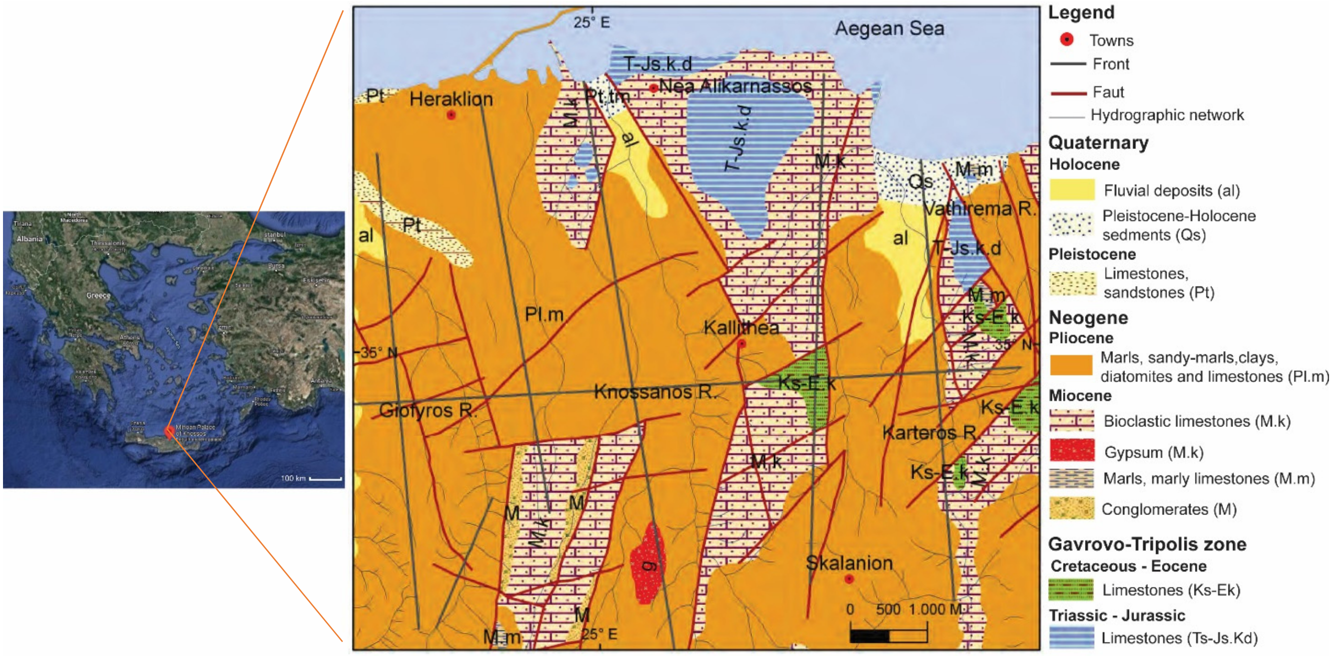

Figure 1. Localization of the Palace of Knossos, Crete, Greece (image/adapted from Google Maps, Maps data © 2021 Google). Geological map of Heraklion region (image/adapted from Kokinou, E. et al. (2013), p. 288 [26]).

Regarding the construction system of the walls, according to Kienzle [29], the constructive techniques used in Knossos could be grouped into three categories described below, although there was a greater predominance of the second category:

> *"The stone work in Knossos falls in three categories. First, there are the ashlar walls which feature a dressed stone surface as at the North Entrance Passage or in the light wells of the Domestic Quarter. Second, there are rubble walls which were constructed with randomly collected undressed stones and were frequently used in combination with a timber framework which will be discussed below. These walls were commonly plastered or covered with gypsum dado slabs. Finally, stone was employed because of its fine surface as paving material, as dado fixed to the wall or as decorative column bases"* [29] (p. 119).

The author also points out the use of "*earth, mud or clay mortars*" in the construction of most of the rubble walls excavated in Knossos [29]. It is worth noticing the importance of supporting wooden structures of built walls that did not survive until the archaeological work performed on the site, making them fragile after excavation. In structures built with clay bricks, many fragments and traces of frescoes were found in various areas, indicating not only the importance of the decoration of the spaces, but also the need for wall protection [4,24,29,32].

The peculiarity of this archaeological site goes beyond its historical richness and gains another dimension with the work carried out by A. Evans and his team in the early 20th century. In different excavation campaigns, it became evident the need to preserve the exposed structures [29]. Initially, they tried to use traditional materials similar to those originally used in the structures. However, this strategy proved ineffective for the protection of these spaces, as the construction techniques used were adequate for covered buildings and not adapted to exterior conditions [29]. In later stages, the option of A. Evans and his team was to rebuild some structures considered important for preservation and fundamental to the understanding of what would be the architectural grandeur of this palace. In the 1920s, they chose to use the most resistant materials existing at the time, namely cement [29,35]. Many of the structures still visitable today are reconstructions based on the remains found during the excavations and on the interpretation of A. Evans and his team. The entire archaeological complex of the Palace of Knossos (Figure 2), including reconstructions, tells a unique history that justifies the study of the materials used and all efforts for their preservation.

(a) (b)

Figure 2. (**a**) Palace of Knossos, view of West Wings; (**b**) View of the north entrance (images: F. Carvalho).

2. Materials and Methods

For the study and characterization of mortars from this archaeological site, samples were collected from visually distinct typologies, with bedding and render functions applied in different locations (Figure 3 and Table 1). Following a minimally invasive approach, the quantity of sample collected in each case was the smallest possible amount necessary for laboratory chemical and morphological analyses, inhibiting the use of some destructive testing techniques such as the acid separation of the binder and the definition of the granulometry of the aggregates via mechanical and/or manual processes.

The samples were prepared in two distinct forms to accommodate the needs of the different analytical techniques. A fragment of each sample was mounted in epoxy resin in their present state and mechanically polished. Additionally, the smallest portion of each sample was grinded on an agate mortar and pestle.

Sample observation was carried out using an Olympus SZ stereo microscope, with a 10× objective and magnification range between 8× to 40× and an Optical Leica DMI5000M microscope in inverted reflected light, in darkfield observation mode, with magnification capacity between 50× and 1000×.

Figure 3. Sampling locations on the Palace of Knossos, West Magazines, and East Wing. (Image adapted from HERACLES Project [3,36]).

Table 1. Samples from the Minoan Palace of Knossos.

Sample	Type of Material	Location
KN-BM1A	Bedding mortar	West Magazines, Magazine IV, south wall (eastern part)
KN-BM2A	Bedding mortar	West Magazines, Magazine IV, south wall (west part)
KN-BM3A	Bedding mortar	East Wing, Hall of Double Axes, south wall
KN-CM1A	Bedding mortar	West Magazines, Magazine V, north wall
KN-CM2A	Bedding mortar	West Magazines, Magazine VI, south wall
KN-CM3A	Bedding mortar	East Wing, Corridor, north wall
KN-CM4A	Bedding mortar	East Wing, Hall of Double Axes, south wall
KN-PL1A	Render mortar	West Magazines, Magazine IV, north wall
KN-PL2A	Render mortar	West Magazines, Magazine IV, north wall
KN-PL3A	Render mortar	East Wing, East-West Corridor, west wall

X-ray fluorescence for chemical analysis was performed using an X-ray fluorescence spectrometer with a wavelength dispersive system (WDXRF) PANalytical–Axios 4.0, with a rhodium X-ray tube (20.21 keV), in conditions optimized for element quantification. The analyzing crystals of LiF220, LiF200, Ge, PE, and PX1 were used for the separation of fluorescent X-ray peaks covering all measurable range. Analysis was performed under He flow and spectra deconvolution using the iterative least-squares method and standardless semiquantitative analysis based on the fundamental parameter approach with the SuperQ IQ+ software package (PANalytical B.V., Almelo, The Netherlands).

X-ray diffraction (XRD) analysis for the identification of mineralogical phases was performed using a Rigaku diffractometer, model DMAX III-C 3kW, with Cu Kα radiation at 40 kV and 30 mA settings, in the 2θ range of 10° to 65°, with a step of 0.08° and an acquisition time of 1 s per step, in continuous scan mode (detection limit under ~4%, in volume [37]). The identification of crystalline phases was carried out using the EVA Software (Bruker AXS GmbH, Karlsruhe, Germany).

Fourier-transform infrared spectroscopy (FTIR) was used as an auxiliary technique in the identification of characteristic vibrations of crystalline phases in inorganic materials and for the identification of any amorphous phases or organic compounds that could be present in the samples. Data was recorded using an attenuated total reflectance (ATR) sampling accessory (Smart iTR) equipped with a single bounce diamond crystal on a Thermo Nicolet 6700 Spectrometer. Spectra were acquired in the range of 4000–525 cm^{-1} and with a 4 cm^{-1} resolution.

Simultaneous thermogravimetry and differential thermal analysis (TG–DTA) for the characterization of thermal processes and mass variation determination of the materials during heating was accomplished with a Setaram TGDTA 92 apparatus using an Ar flow with a heating rate up to 1100 °C of 10 °C/min. Although it is a destructive technique, the amount of sample used corresponds to a micrometric volume of 50 µL, in this case, 0.042 to 0.065 g of sample, which was considered acceptable in the present experimental conditions.

3. Results and Discussion

The set of samples from the Palace of Knossos reveals the diversity that mortars can achieve, even when used for the same function. The observation of the samples as-received highlights that the set of bedding mortar samples, designated by KN-BM1A, BM2A, and BM3A, were very loose, being necessary to select the aggregate parts of each sample to assemble in resin. All samples were observed in cross section under an optical microscope with the same magnification of 50× (Figure 4).

By optical microscope observation, although it is not possible to point out a common morphological pattern for all samples it is noticeable that the mortars used as bedding of stonework are similar in characteristics between them and distinct from the group of samples used as coatings (render samples).

Four of the bedding mortar samples come from the West Magazines. KN-BM1A (Figure 4a) and KN-BM2A (Figure 4b) samples come from the same side of the wall, taken at opposite ends, both at the top. KN-CM1A (Figure 4d) and KN-CM2A (Figure 4e) samples are from opposite sides of the same wall dividing warehouses IV and V, collected from cohesive parts, both from an interior area corresponding to the support beams, and from a more exposed area of the wall. The two first-referred samples show stronger disaggregation when compared to the other two samples in the set. The top of the image in sample KN-BM1A, when observed in cross section (Figure 4a), corresponds to the coarsest aggregates used for the formulation of the mortar. It is a carbonated rock with foraminifera bioclasts with different shapes. The bottom of Figure 4a corresponds to a cohesive part of the binder, with thin aggregates, ranging from 0.06 to 0.30 mm, well distributed in the binder. At the opposite end of the same structure, the KN-BM2A cross section sample corresponds to a well-compacted zone of the binder, with fine aggregates, composed of more angled grains, ranging from 0.06 to 0.50 mm. The binder has a pinkish hue and more homogeneous distribution of aggregates. The samples KN-CM1A and KN-CM2A, both from joints of different walls of the West Magazines, present the typical characteristic visual binder color of a clayey material. Both have well-distributed aggregates, ranging from 0.06 to 0.80 mm, although the KN-CM2A sample presents a more homogeneous distribution and a lower visible porosity. The samples used as bedding mortars that show greater morphological variations were collected in the East Wing of the archaeological site in different rooms, corresponding to the reconstructions area promoted by A. Evans and his team, both in terms of binder characteristics and distribution of aggregates. From this set, sample KN-BM3A (Figure 4c) presents the binder with the characteristic shade of clayey materials, exhibiting a stronger red color and being darker than binder samples from the West Magazine. The aggregates are distributed more irregularly, and its constituents are mostly rounded and fine-grained, with a greyish shade common on silicate sands. Some of the coarser grains also present have a reddish color and correspond to hematite. The binder presents visible pores and fissures. The KN-CM4A sample (Figure 4g) presents fine-grained angled aggregate particles, with a heterogeneous mineralogy. The binder has a pink coloration, as in the KN-BM1A sample, but shows some cracking. The KN-CM3A sample (Figure 4f), also collected in the East Wing, presents the highest cracking of the binder (remaining cohesive). The aggregates show distinct and irregular shapes, with predominance of elongated and angled grains, corresponding to silicate sands. It is possible to observe fragments of foraminifera, as observed in sample KN-BM1A, although scarcer in number. The presence of foraminifera bioclasts in the samples may indicate the use of local raw material, as in the Knossos region there are predominant areas of bioclastic limestones (see Figure 1).

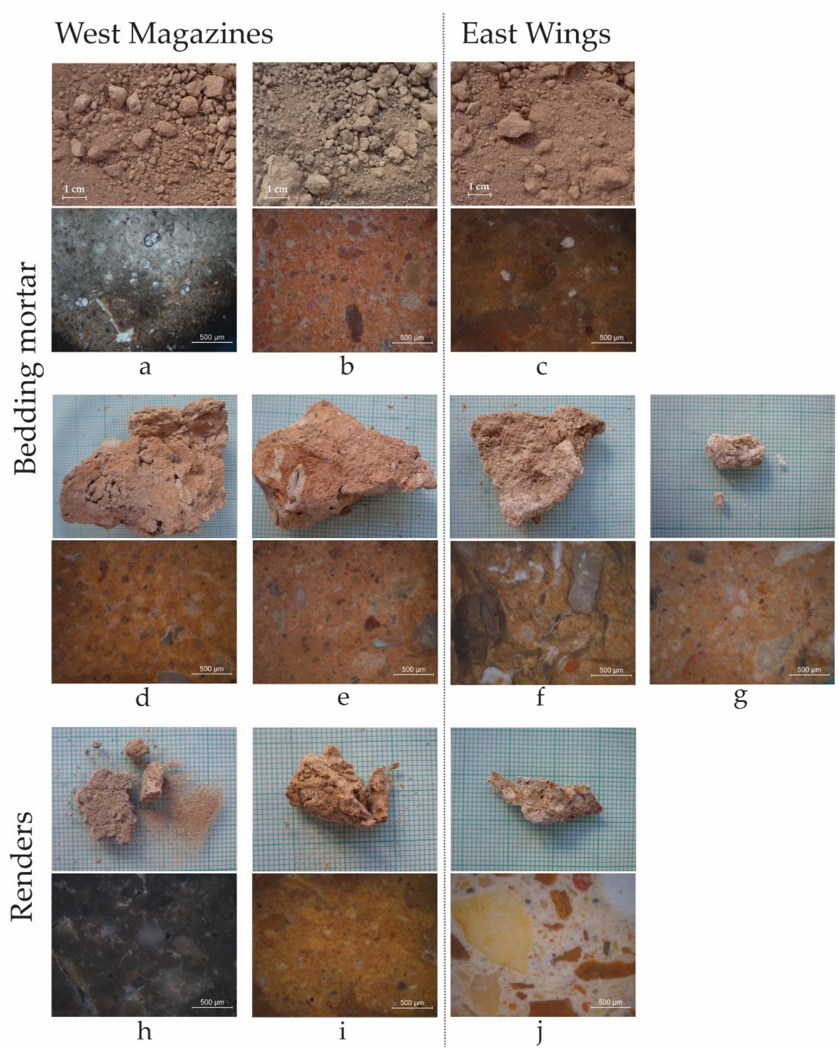

Figure 4. Set of samples from the Palace of Knossos, both as-received and in polished section observation. Bedding mortar samples from West Magazines (**a**) KN-BM1A; (**b**) KN-BM2A; (**d**) KN-CM1A; (**e**) KN-CM2A. Bedding mortar from East Wing (**c**) KN-BM3A; (**f**) KN-CM3A; (**g**) KN-CM4A. Render samples from West Magazines (**h**) KN-Pl1A; (**i**) KN-Pl2A; render sample from East Wing (**j**) KN-Pl3A.

The samples taken from renders also show a great variation in their characteristics. Samples KN-Pl1A and KN-Pl2A (Figure 4h,i) from the West Magazines have a binder with different colorations, pores, and cracks. KN-Pl1A presents more cracking and coarser grains heterogeneously dispersed, and a darker binder, which hinders the observation of the finer-grained aggregates under optical microscopy. The KN-Pl2A sample, with a pinkish/reddish binder earthy hue typical of clay materials, has mostly fine aggregates, with an average size between 0.06 and 0.40 mm, distributed heterogeneously. Predominantly, light-colored finer-grained quartz occurs, while larger grains are mostly opaque reddish in color. There are also fragments of foraminifers with different shapes. Sample KN-Pl3A is the one with the greatest differences in this set, with a clear, microgranulated, and very cohesive binder, and aggregates with fine, medium, and coarse particles, well distributed throughout the sample. The grains are angled and of distinct hues, due to a greater mineralogical diversity. Table 2 presents a summary of the main characteristics of the samples observed in cross-section by optical microscope.

The bulk chemical composition of each sample was determined by WDXRF, and the results obtained, expressed in oxides (wt%), are presented in Table 3. All samples show high percentages of Ca and Si, except KN-CM3A, which has the lowest percentage of Si of the set. It should be noted that it also has the highest percentage of S. The results reveal that the mortars used as bedding in the West Wing present more regular compositions. The greatest differences in composition correspond to the set of samples collected in the East Wing. In this case, the mortars used for joining show the greatest variations in relation to the percentages of Si and S.

Render mortar samples have high percentages of Ca and low percentages of Si, with KN-Pl1A showing extreme values for each of these elements. They also have lower percentages of Al. Sample KN-Pl2A from the West Wing has a higher S content, being the only sample richer in this element when considering the set of render samples. The overall composition of this sample is similar to bedding samples from the same structure.

Table 2. Summary of the main characteristics of mortars observed by OM in cross section.

	Samples	Function	Binder		Aggregates		Other Observations
			Cohesion	**Hue Color (Average RGB)**	**Particle-Size (mm)**	**Distribution**	
West Magazine	KN-BM1A	Bedding	No	143, 111, 63	0.06 to 0.30	Homogeneous	Foraminifera bioclasts
	KN-BM2A		No	185, 111, 54	0.06 to 0.50	Homogeneous	Foraminifera bioclasts
	KN-CM1A		Yes	174, 104, 34	0.06 to 0.50	Heterogeneous	Visible porosity and cracks
	KN-CM2A		Yes	189, 123, 58	0.07 to 0.80	Homogeneous	Visible porosity
	KN-Pl1A	Renders	Yes	63, 55, 48	0.10 to 0.50	Heterogeneous	Visible porosity and cracks
	KN-Pl2A		Yes	179, 119, 46	0.06 to 0.40	Heterogeneous	Foraminifera bioclasts; visible porosity and cracks
East Wing	KN-BM3A	Bedding	No	133, 87, 40	0.09 to 0.70	Heterogeneous	Foraminifera bioclasts; visible porosity and cracks
	KN-CM3A		Yes	188, 140, 76	0.10 to 0.50	Heterogeneous	Foraminifera bioclasts; visible porosity and cracks
	KN-CM4A		Yes	187, 134, 65	0.06 to 0.08	Homogeneous	Visible porosity and cracks
	KN-Pl3A	Renders	Yes	215, 190, 152	0.06 to 2.10	Heterogeneous	Foraminifera bioclasts; visible porosity

Table 3. Chemical composition of mortar samples from the Palace of Knossos, obtained by WDXRF (wt%) ("-" not detected).

	Samples	Function	CaO	SiO_2	Al_2O_3	Fe_2O_3	MgO	K_2O	Na_2O	P_2O_5	TiO_2	SO_3	Cl	SrO	MnO
West Magazine	KN-BM1A	Bedding	53.39	29.15	7.27	4.94	2.16	1.26	-	0.57	0.62	0.41	0.06	0.08	0.08
	KN-BM2A		51.29	28.45	7.11	6.21	2.19	1.32	1.24	0.64	0.66	0.59	0.14	0.08	0.07
	KN-CM1A		48.97	32.34	7.95	5.34	1.65	1.24	-	0.79	0.68	0.54	0.21	0.11	0.09
	KN-CM2A		45.97	36.06	8.32	5.24	1.54	1.17	-	0.46	0.60	0.36	0.09	0.08	0.11
	KN-Pl1A	Renders	86.02	7.25	2.05	1.02	1.46	0.32	-	-	0.19	0.46	1.14	0.06	0.04
	KN-Pl2A		53.47	23.83	6.61	3.93	2.12	1.19	-	0.13	0.51	8.04	0.04	0.07	0.07
East Wing	KN-BM3A	Bedding	48.76	28.74	7.55	4.79	2.41	1.56	-	0.77	0.59	4.41	0.27	0.07	0.07
	KN-CM3A		43.79	13.20	2.97	2.06	1.61	1.49	-	0.24	0.21	33.60	0.47	0.32	0.04
	KN-CM4A		39.19	36.49	7.72	3.21	2.28	0.61	6.29	-	0.46	2.87	0.78	0.04	0.07
	KN-Pl3A	Render	64.12	18.21	4.89	2.39	3.44	1.01	1.37	-	0.27	4.04	0.15	0.06	0.05

Semiquantification of the main mineral phases identified by XRD analysis are presented in Table 4. Calcite and quartz were identified in all samples, with predominance of calcite, except in KN-CM3A, where gypsum peaks are more intense, consistent with the high percentage of S shown in Table 3. Despite the differences in characteristics of binders and aggregates observed by optical microscopy in the samples collected in the West Magazines, XRD and WDXRF results indicate a greater similarity in the mineralogical and chemical composition of these samples, especially in bedding samples from the same wall structure. On the other hand, samples collected in the East Wing of the archaeological site present a greater variety in mineralogical composition, having been identified in addition to calcite and quartz (the two with the more intense peaks), and other minerals, such as albite, dolomite, gypsum, siderite, hematite, and gehlenite.

Table 4. Main crystalline phases identified by XRD in the samples of the Palace of Knossos. Calcite ($CaCO_3$), quartz (SiO_2), albite ($Na[AlSi_3O_8]$), gypsum ($CaSO_4{\cdot}2H_2O$), hematite (Fe_2O_3), dolomite ($CaMg[CO_3]_2$), siderite ($FeCO_3$), and gehlenite ($Ca_2Al[AlSi]O_7$) (see Supplementary Material).

	Sample	Function	Main Mineral Phases Identified
West Magazine	KN-BM1A	Bedding	Calcite (++++), quartz (++), albite *
	KN-BM2A		Calcite (++++), quartz (++), albite *
	KN-CM1A		Calcite (++++), quartz (++)
	KN-CM2A		Calcite (++++), quartz (+++)
	KN-Pl1A	Renders	Calcite (++++), quartz *
	KN-Pl2A		Calcite (++++), quartz (++), gypsum (+), albite *
East Wing	KN-BM3A	Bedding	Calcite (++++), quartz (+++), hematite *
	KN-CM3A		Gypsum (++++), calcite (+++), quartz (+++), dolomite (++), siderite *
	KN-CM4A		Calcite (++++), quartz (++), hematite *
	KN-Pl3A	Render	Calcite (++++), quartz (+), dolomite *, gehlenite *

* Low-intensity peaks; (+) to (++++) indicates XRD peak relative intensity from weak to strong.

The FTIR-ATR results confirm the main mineral phases identified by XRD, with the most intense vibration bands observed in the spectra attributed to the same minerals. All results obtained by FTIR-ATR are characteristic of inorganic materials, and no band corresponding to the presence of organic materials or contaminants has been identified. The difference between the spectra is mainly in the widening of some bands, especially those centered in the fingerprint area, where it is common to overlap characteristic bands of different ion groups [38]. All samples present the characteristic vibration of calcium carbonate, with the extended stretching band of the group CO_3^{2-} to vary between 1413 and 1394 cm^{-1} and the narrow bending bands of the carbonate group centered on 874–872 cm^{-1} and 712 cm^{-1} [39–41]. The characteristic vibration bands of the group Si–O–Si, wider and centered on 1010 and 1003 cm^{-1}, and the narrower and less intense bands, centered

798 and 779 cm^{-1}, attributed to quartz [39,41], are also present in all spectra, being less pronounced in the results obtained for KN-PL1A, where calcite vibrations predominate, as was also observed in XRD results. The results obtained for sample KN-CM3A, from the East Wing of the archaeological site, show predominance of the vibration bands characteristic of dihydrated calcium sulfate, with the stretching vibration bands of the group OH at 3531, 3400, and 3242 cm^{-1}, the bending bands of the group OH centered at 1683 and 1620 cm^{-1}, and the stretching band of the sulfate ion SO_4^{2-} centered at 1109 cm^{-1} and 667 cm^{-1} [40,42]. The spectrum also features the characteristic bands of carbonate ion CO_3^{2-}, calcium carbonate, as well as the characteristic bands of Si–O vibrations attributed to quartz, as observed with XRD.

The results confirm the similarity of the composition of the samples collected in the West Magazines, especially for bedding mortars (Figure 5a), consistent with XRF and XRD analysis. Considering that the samples were collected in structural traces of the same wall, but on opposite sides, this similarity indicates that the studied samples were collected from mortars apparently prepared and applied in the same period, even if they present some differences in appearance when observed in situ. Bedding samples from the East Wing of Palace of Knossos (Figure 5b) show more variations among themselves, similarly to the results obtained in the previous analyses. It is important to highlight that the reconstruction work promoted by A. Evans and his teams was carried out in different stages between 1905 and 1930, approximately, under the coordination of different architects. The work methodology and materials used for these constructions were changed and adapted to better meet the preservation needs of archaeological structures, according to the technical knowledge of the teams, the availability of materials, and the way of thinking in the beginning of the 20th century, marked by war. Therefore, this observed variation in samples from the East Ward may be associated with several factors related to the historical context and the construction process itself. Results from samples of mortars with render function (Figure 5c) are consistent with the mineral phases identified by XRD, with the vibration bands of the carbonate group attributed to calcium carbonate, and Si–O vibration bands attributed to quartz. FTIR-ATR results of the KN-PL3A sample also present the vibration bands referring to the sulphate group (SO_4^{2-}) at 1100 and 667 cm^{-1}, together with OH group vibration bands at 3534, 3400 cm^{-1}, and 1620 cm^{-1}, which indicates the presence of gypsum, although this mineral phase was not identified by XRD.

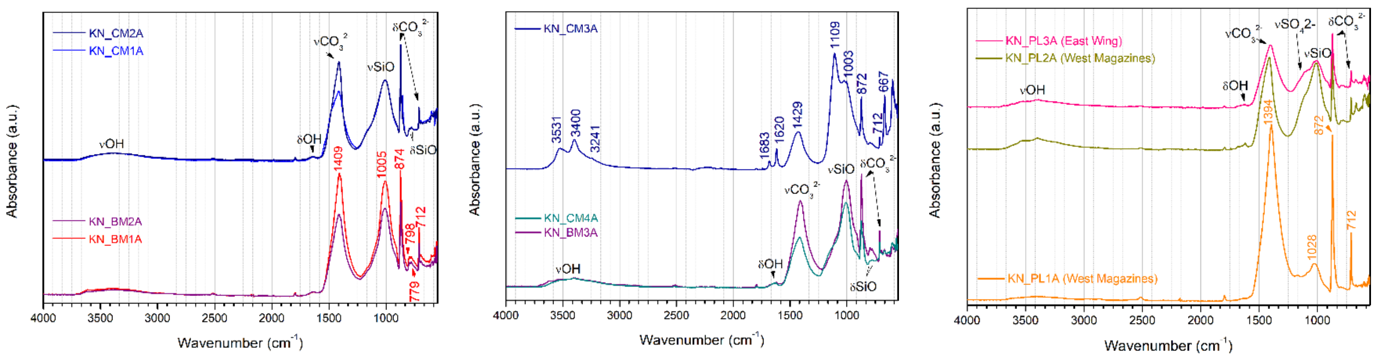

(**a**) (**b**) (**c**)

Figure 5. FTIR spectra for samples collected at Knossos Palace: (**a**) results of the bedding samples of west magazines; (**b**) results of East Wing bedding samples; (**c**) results of samples with render function.

Simultaneous thermogravimetry and differential thermal analysis was performed only in mortars from bedding stonework, respecting the amount of sample available as it is a destructive technique. The mass losses were calculated from the data obtained from the thermogravimetric curves (TG) (Figure 6b) and are presented in Table 5. The curves obtained by differential thermal analysis (DTA) (Figure 6a) show endothermic peaks up to 200 °C for all samples, attributed to the loss of adsorbed water compatible with nonhydrated compounds, except in the KN-CM3A sample where the DTA curve is characteristic of dihydrated calcium sulfate, with two endothermic peaks with maximums at 87 °C and 175 °C, corresponding to the loss of hydration water [43,44]. In addition, the curve also presents an exothermic peak with a maximum of 422 °C attributed to the change of the crystalline structure from anhydrite I to anhydrite II [43,44]. All samples show the same tendency of mass loss, from 600 °C, with the maximum ranging between 800 and 900 °C, attributed to the transformation of calcium carbonate. In this case, the calculated mass loss (Table 5) varies between 9.29% and 24.44%, the lowest loss corresponding to sample KN-CM3A, indicating that this mortar has gypsum as the main binder. Sample KN-CM4A shows the highest percentage of mass loss calculated between 200 and 600 °C, attributed to the structural water losses of the compounds [45].

Table 5. Results obtained by TG–DTA: mass loss of water, of CO_2 and CO_2/H_2O ratio.

Sample	H_2O Loss (%)			CO_2 Loss (%)	Total Loss (%)	CO_2/H_2O
	<120 °C	120–200 °C	200–600 °C			
KN_BM1A	0.53	0.47	2.23	24.44	27.67	10.98
KN_BM3A	0.69	0.60	2.73	21.86	25.89	8.00
KN_CM2A	0.88	1.11	3.63	19.07	24.69	5.26
KN_CM3A	1.10	3.11	2.62	9.29	16.12	-
KN_CM4A	1.66	1.52	5.09	18.12	26.38	3.56

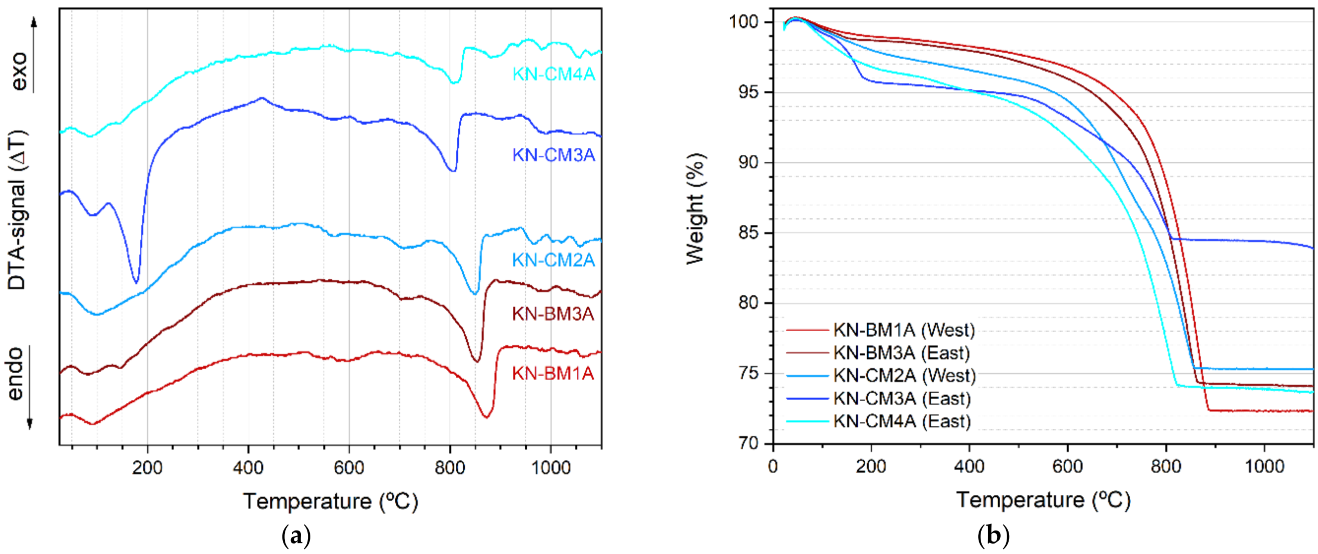

Figure 6. TG–DTA curves of mortar samples from the Palace of Knossos: (**a**) comparison of the curves obtained by differential thermal analysis, in which the curve referring to the KN-CM3A sample stands out, with the endothermic peak characteristic of dihydrate calcium sulfate; (**b**) comparison of the curves resulting from the thermogravimetric analysis, in which the similar trend for percentage of weight loss to all samples stands out, except for the KN-CM3A sample.

When considering the CO_2/H_2O loss ratio in Table 5, calculated from TG values, the degree of hydraulicity of the mortar can be inferred, because the lower the value of this ratio, the greater the degree of hydraulicity of the mortar. The literature considers that ratios above 10 correspond to aerial lime mortars, while the values between 3.5 and 10 are considered hydraulic mortars, and below 3.5 are considered pozzolans [10,46–48]. Based on the values obtained, it is possible to observe that KN-BM1A presents a value compatible with that of an aerial mortar, and the other mortars present values corresponding to hydraulic mortars. In the case of sample KN-CM3A, it is important to note that all the results indicate and confirm that it is gypsum-based (non-lime-based), and this sample was therefore disregarded as this ratio is considered as an indicator of hydraulicity for lime-based mortars.

4. Conclusions

The study of the mortar samples collected at the Palace of Knossos revealed differences in compositions in relation to the function of the material, as expected, but also regarding its location in the archaeological site. In addition, the results obtained in this study are consistent with the mineralogy of the region, which may indicate the use of local raw material for the formulation of mortars. The bedding mortars samples presented greater similarity in chemical and mineralogical composition, especially for the samples from the West Magazines. In this case, the similarity from results obtained with all techniques is evident, pointing to the use of lime-based mortars, with mineralogical predominance of calcite and quartz for all West Magazines samples and, in addition to these minerals, the presence of plagioclase (XRD-determined albite) in the samples from the same side of the wall. However, the degree of hydraulicity calculated by TG–DTA shows some differences, indicating values corresponding to, or closer to, air lime mortar for the bedding samples from the same side of the wall and values corresponding to hydraulic lime for samples from the opposite side of the wall. Considering that these set of samples come from the wall that divides warehouses IV and V, this similarity in compositions observed in all results is consistent with a construction resulting from the same workforce, probably carried out in the same period, although it is difficult to determine what this period would be.

Regarding the bedding mortar samples from the east side of the Palace of Knossos, the results reflect a greater variation in chemical and mineralogical composition. Of the three samples studied, two correspond to lime-based mortars, with the predominance of calcite and quartz as the main mineral components, and one corresponds to a gypsum-based mortar. When compared to the samples from the West Magazines, this set presented a higher variety of minerals identified by XRD, and also a greater variation in the percentage of the most abundant chemical elements. It is important to interpret these results bearing in mind that these samples were collected in different structures in the area reconstructed and/or intervened by the A. Evans team, and the results reflect a distinct constructive approach. The variation in composition may indicate different phases of work and even of materials and preparation techniques, consistent with the extent of the work developed at the beginning of the 20th century. It is also worth mentioning that the works carried out by A. Evans and his team were made over more than 30 years, in periods interrupted by wars, which may partly explain the difference in composition observed in the materials used for joining blocks.

Regarding the results obtained for the render samples, it is possible to observe a greater variation in chemical and mineralogical compositions, even in samples from the West Magazines. All samples showed the highest calcium content obtained by WDXRF, and calcite and quartz were identified as the predominant minerals, in addition to other constituents. The main differences are observed by optical microscopy regarding granulometry and grain shape in each of the samples. It is important to emphasize that renders are generally applied in layers and that aggregate granulometry is fundamental for material performance. As in bedding samples, the characteristics observed in the render samples from the East Ward show a clear difference in the material produced and applied in the reconstruction phase of the Palace, in relation to the samples from the nonreconstructed West Magazines.

The study of the mortar samples collected at the Palace of Knossos revealed differences in compositions in relation to the function of the material, as expected, but also regarding its location in the archaeological site. It is important to emphasize that, often, due to the historical importance of a monument, studies are limited by the amount of sample collected and the impossibility of new sampling campaigns. For this reason, we opted for the methodological approach proposed in this study, which favored nondestructive techniques or that required the least possible sample in the case of destructive techniques.

This approach has brought some limitations in relation to the choice of techniques and interpretation of the results. As a future perspective, it would be of interest to include other nondestructive techniques, such as Raman and SEM for the characterization of the aggregate and the binder, without the need to physically separate the binder from the aggregate. Nevertheless, with this study, a further step is made into bridging historical knowledge and present-day comprehension of these complex materials, contributing to interpretation of their characteristics.

Supplementary Materials: The following are available online at https://www.mdpi.com/article/10.3390/min12010030/s1, Figure S1: XRD diffractmeters.

Author Contributions: Conceptualization, investigation, and writing: F.C. and J.P.V.; methodology: F.C., J.P.V. and G.P.; formal analysis: F.C., N.L., J.S., T.P.d.S. and J.P.V.; data curation: E.K.; writing—original draft preparation: F.C. and P.S.; writing—review and editing: F.C., J.P.V., N.L., J.S., E.K., T.P.d.S. and G.P.; visualization: M.M.L. and H.Á.; supervision: J.P.V.; project administration: G.P and J.P.V.; funding acquisition: G.P. and J.P.V. All authors have read and agreed to the published version of the manuscript.

Funding: This research was funded by FEDER funds through the COMPETE 2020 Programme and National Funds through FCT-Portuguese Foundation for Science and Technology under the project ref. UIDB/50025/2020-2023 and, SFRH/BD/145308/2019 (F. Carvalho). The funding from the European Union Horizon 2020 research and innovation programme H2020-DRS-2015 GA nr. 700395 (HERACLES project) and funding from the European Institute of Innovation and Technology (EIT), a body of the European Union, under Horizon 2020, the EU Framework Programme for Research and Innovation, through the MineHeritage Project (PA 18111).

Acknowledgments: The authors would like to thank Eleni Kokinou, of Hellenic Mediterranean University, for the permission to use the image, originally published in the article "Kokinou, E.; Skilodimou, H.; Bathrellos, G. Morphotectonic analysis of Heraklion Basin (Crete, Greece). *Bull. Geol. Soc. Greece* **2013**, *47*, pp. 288".

Conflicts of Interest: The authors declare no conflict of interest.

References

1. Brimblecombe, P. Air Pollution and Architecture: Past, Present and Future. *J. Arch. Conserv.* **2000**, *6*, 30–46. [CrossRef]
2. Alexandrakis, G.; Manasakis, C.; Kampanis, N.A. Economic and Societal Impacts on Cultural Heritage Sites, Resulting from Natural Effects and Climate Change. *Heritage* **2019**, *2*, 279–305. [CrossRef]
3. Padeletti, G. (Coord) HERACLES Project. Available online: http://www.heracles-project.eu/project/project-objectives (accessed on 14 January 2019).
4. Hatzigiannakis, K.; Melessanaki, K.; Philippidis, A.; Kokkinaki, O.; Kalokairinou, E.; Siozos, P.; Pouli, P.; Politaki, E.; Psaroudaki, A.; Dokoumetzidis, A.; et al. Monitoring and Mapping of Deterioration Products on Cultural Heritage Monuments Using Imaging and Laser Spectroscopy. *Commun. Comput. Inf. Sci.* **2019**, *962*, 419–429. [CrossRef]
5. Veiga, R. Air lime mortars: What else do we need to know to apply them in conservation and rehabilitation interventions? A review. *Constr. Build. Mater.* **2017**, *157*, 132–140. [CrossRef]
6. Artioli, G.; Secco, M.; Addis, A. The Vitruvian legacy: Mortars and binders before and after the Roman world. *Contrib. Mineral. Cult. Herit.* **2019**, *20*, 151–202. [CrossRef]
7. Crisci, G.M.; Franzini, M.; Lezzerini, M.; Mannoni, T.; Riccardi, M.P. Ancient mortars and their binder. *Period. Miner.* **2004**, *73*, 259–268.
8. Rodríguez-Navarro, C. Binders in historical buildings: Traditional lime in conservation. *Semin. SEM* **2012**, *9*, 91–112.
9. Santos, A.R.; Veiga, M.D.R.; Silva, A.S.; de Brito, J.; Álvarez, J.I. Evolution of the microstructure of lime based mortars and influence on the mechanical behaviour: The role of the aggregates. *Constr. Build. Mater.* **2018**, *187*, 907–922. [CrossRef]
10. Elsen, J. Microscopy of historic mortars—A review. *Cem. Concr. Res.* **2006**, *36*, 1416–1424. [CrossRef]
11. Young, R. Lime-Based Plasters, Renders and Washes. In *Materials & Skills for Historic Building Conservation*; Wiley: Hoboken, NJ, USA, 2008; pp. 56–91.
12. Arizzi, A.; Cultrone, G. The influence of aggregate texture, morphology and grading on the carbonation of non-hydraulic (aerial) lime-based mortars. *Q. J. Eng. Geol. Hydrogeol.* **2013**, *46*, 507–520. [CrossRef]
13. Elsen, J.; Van Balen, K.; Mertens, G. *Historic Mortars*; Válek, J., Hughes, J.J., Groot, C.J.W.P., Eds.; RILEM Bookseries; Springer: Dordrecht, The Netherlands, 2012; Volume 7, ISBN 978-94-007-4634-3.
14. Budak, M.; Maravelaki-Kalaitzaki, P.; Kallithrakas-Kontos, N. Chemical characterization of Cretan clays for the design of restoration mortars. *Microchim. Acta* **2008**, *162*, 325–331. [CrossRef]

15. Arizzi, A.; Cultrone, G. Mortars and plasters—How to characterise hydraulic mortars. *Archaeol. Anthr. Sci.* **2021**, *13*, 144. [CrossRef]
16. Veiga, M.D.R.; Fragata, A.; Velosa, A.; Magalhães, A.C.; Margalha, G. Lime-Based Mortars: Viability for Use as Substitution Renders in Historical Buildings. *Int. J. Arch. Herit.* **2010**, *4*, 177–195. [CrossRef]
17. Stefanidou, M.; Papayianni, I. The role of aggregates on the structure and properties of lime mortars. *Cem. Concr. Compos.* **2005**, *27*, 914–919. [CrossRef]
18. Ellis, S.; Lawrence, M.; Walker, P. A Critical Review of the Effect of Calcitic Aggregate on Air Lime Mortar. *Int. Congr. Mater. Struct. Stab.* **2013**, *5*, 97.
19. Veiga, R. *Conservação e Reparação de Revestimentos de Paredes de Edifícios Antigos—Métodos e Materiais*; LNEC: Lisboa, Portugal, 2009; ISBN 9789724921761.
20. Figueiredo, M.O.; Veiga, J.P.; Silva, T.P. Materials and reconstruction techniques at the Aqueduct of Carthage since the Roman period. In *Historical Constructions*; Universidade do Minho: Guimarães, Portugal, 2001; pp. 391–400.
21. Palomo, A.; Blanco-Varela, M.T.; Martinez-Ramirez, S.; Puertas, F.; Fortes, C. Historic mortars: Characterization and durability, new tendencies for research. In *Fifth Framework Programme Workshop, Prague*; CORDIS EU: Brussels, Belgium, 2002.
22. Fabio, S.; Massimo, B.; Stefano, C.; Carla, L.; Catarina, M.; José, M. Ancient restoration and production technologies of Roman mortars from monuments placed in hydrogeological risk areas: A case study. *Archaeol. Anthr. Sci.* **2020**, *12*, 147. [CrossRef]
23. Elissavet, K.; Dokoumetzidi, A.; Kanaki, E.; Katsaveli, E.; Politaki, E. The Palace of Knossos and the Venetian Fortress «Rocca a Mare» (Koules) in Heraklion, Crete, Greece: How the HERACLES activities and platform will contribute to their protection and resilience against climatic events. In Proceedings of the EGU General Assembly 2018, Vienna, Austria, 8–13 April 2018.
24. Knossos Scientific Committee. *Knossos 2000–2008. Conservation, Consolidation and Promotion of the Palace and Archaeological Site*; Knossos Scientific Committee: Heraklion, Greece, 2008.
25. Hood, S.; Smyth, D. Archaeological survey of the Knossos Area. *Br. Sch. Athens. Suppl. Vol.* **1981**, *14*, 1–69. [CrossRef]
26. Kokinou, E.; Skilodimou, H.D.; Bathrellos, G.D. Morphotectonic analysis of Heraklion Basin (Crete, Greece). *Bull. Geol. Soc. Greece* **2016**, *47*, 285–294. [CrossRef]
27. Fassoulas, C. The geological setting of Crete: An overview. In *Minoan Earthquakes—Breaking the Myth Through Interdisciplinarity*; Jusseret, S., Sintubin, M., Eds.; Leuven University Press: Leuvain, Belgium, 2017; pp. 135–164. ISBN 978 94 6270 105 2.
28. Roberts, N. The Location and Environment of Knossos. *Annu. Br. Sch. Athens* **1979**, *74*, 231–241. [CrossRef]
29. Kienzle, P. Conservation and reconstruction at the Palace of Minos at Knossos Seminar at the University of York, 1996. *Conserv. Manag. Archaeol. Sites* **1997**, *2*, 121–124. [CrossRef]
30. MacDonald, C. Knossos. In *The Oxford Handbook of the Bronze Age Aegean*; Oxford University Press: Oxford, UK, 2012; pp. 1–14. [CrossRef]
31. Driessen, J. The Central Court of the Palace of Knossos. *Br. Sch. Athens Stud.* **2004**, *12*, 75–82.
32. Evans, A.J. The Palace of Knossos. *Annu. Br. Sch. Athens* **1901**, *7*, 1–120. [CrossRef]
33. Evans, A. *The Palace of Minos at Knossos*; Macmillan and Co.: London, UK, 1921; Volume I.
34. Graham, J.W. The Residential Quarter of the Minoan Palace. *Am. J. Archaeol.* **1959**, *63*, 47–52. [CrossRef]
35. Evans, A. Work of Reconstitution in the Palace of Knossos. *Antiq. J.* **1927**, *7*, 258–267. [CrossRef]
36. Padeletti, G.; Curulli, A. Deliverable D1.2—Milestone MS1—Definition of the End Users Requirements with Emphasis on HERACLES Test-Beds. 2018. Available online: http://www.heracles-project.eu/ongoing/achievements (accessed on 3 November 2021).
37. Vyverberg, K.L.; Jaeger, J.M.; Dutton, A. Quantifying Detection Limits and Uncertainty in X-ray Diffraction Mineralogical Assessments of Biogenic Carbonates. *J. Sediment. Res.* **2018**, *88*, 1261–1275. [CrossRef]
38. Chukanov, N.V.; Chervonnyi, A.D. *Infrared Spectroscopy of Minerals and Related Compounds*; Springer International Publishing: Berlin/Heidelberg, Germany, 2016.
39. Reig, F.B.; Adelantado, J.V.G.; Moreno, M.C.M.M. FTIR quantitative analysis of calcium carbonate (calcite) and silica (quartz) mixtures using the constant ratio method. Application to geological samples. *Talanta* **2002**, *58*, 811–821. [CrossRef]
40. Derrick, M.R.; Stulik, D.; Landry, J.M. *Infrared Spectroscopy in Conservation Science*; Ball, T., Tidwell, S., Ge, P.J., Eds.; Getty Publications: Los Angeles, CA, USA, 1999; ISBN 0892364696.
41. Medeghini, L.; Mignardi, S.; De Vito, C.; Conte, A.M. Evaluation of a FTIR data pretreatment method for Principal Component Analysis applied to archaeological ceramics. *Microchem. J.* **2016**, *125*, 224–229. [CrossRef]
42. Socrates, G. *Infrared and Raman Characteristic Group Frequencies: Tables and Charts*; John Wiley & Sons: Chichester, UK, 2001.
43. Engbrecht, D.C.; Hirschfeld, D.A. Thermal analysis of calcium sulfate dihydrate sources used to manufacture gypsum wallboard. *Thermochim. Acta* **2016**, *639*, 173–185. [CrossRef]
44. Adams, J.; Kneller, W.; Dollimore, D. Thermal analysis (TA) of lime- and gypsum-based medieval mortars. *Thermochim. Acta* **1992**, *211*, 93–106. [CrossRef]
45. Bakolas, A.; Biscontin, G.; Moropoulou, A.; Zendri, E. Characterization of structural byzantine mortars by thermogravimetric analysis. *Thermochim. Acta* **1998**, *321*, 151–160. [CrossRef]
46. Corti, C.; Rampazzi, L.; Bugini, R.; Sansonetti, A.; Biraghi, M.; Castelletti, L.; Nobile, I.; Orsenigo, C. Thermal analysis and archaeological chronology: The ancient mortars of the site of Baradello (Como, Italy). *Thermochim. Acta* **2013**, *572*, 71–84. [CrossRef]

47. Moropoulou, A.; Bakolas, A.; Bisbikou, K. Investigation of the technology of historic mortars. *J. Cult. Heritage* **2000**, *1*, 45–58. [CrossRef]
48. Carvalho, F.; Lopes, A.; Curulli, A.; Da Silva, T.P.; Lima, M.M.R.A.; Montesperelli, G.; Ronca, S.; Padeletti, G.; Veiga, J.P. The Case Study of the Medieval Town Walls of Gubbio in Italy: First Results on the Characterization of Mortars and Binders. *Heritage* **2018**, *1*, 468–478. [CrossRef]